IMF clock angle control of multifractality in ionospheric velocity fluctuations

G. A. Abel,[1] M. P. Freeman,[1] and G. Chisham[1]

Received 31 July 2009; accepted 25 August 2009; published 7 October 2009.

[1] We present an analysis of 8 years of meridional line-of-sight ionospheric plasma velocity measurements from the Halley SuperDARN radar which investigates the effect of the interplanetary magnetic field (IMF) clock angle on the scaling exponents of the first three order velocity structure functions. We only use velocity measurements made poleward of the open/closed magnetic field line boundary in the nightside ionosphere. The measured scaling exponents are consistent with multifractal Kraichnan-Iroshnikov turbulence for all clock angles but with varying intermittency that decreases to zero during purely northward IMF conditions. We thus propose that intermittency is inherited from the solar wind but also discuss other possible reasons for this relationship. **Citation:** Abel, G. A., M. P. Freeman, and G. Chisham (2009), IMF clock angle control of multifractality in ionospheric velocity fluctuations, *Geophys. Res. Lett.*, *36*, L19102, doi:10.1029/2009GL040336.

1. Introduction

[2] Since the realization of *Dungey* [1961] that convection in the magnetosphere-ionosphere (M-I) system is driven by the solar wind through magnetic reconnection, a large body of work has developed to understand its details. This convection, and the effect of different interplanetary magnetic field (IMF) conditions on its intensity and morphology, is now largely understood at the global scale. More recently there has been interest in understanding the dynamics of the system over a range of scales in a statistical (rather than phenomenological) framework. Many such studies have demonstrated the existence of scale-free structure, i.e., a probability distribution or power spectrum of fluctuations with no characteristic scales (power law) over a wide range of scales. Examples include studies of ground magnetic fields [*Campbell*, 1976; *Francia et al.*, 1995; *Consolini et al.*, 1998; *Weatherwax et al.*, 2000; *Abel and Freeman*, 2002; *Pulkkinen et al.*, 2006], ionospheric electric fields [*Bering et al.*, 1995; *Buchert et al.*, 1999; *Abel and Freeman*, 2002], the geomagnetic indices AU, AL and PC [*Takalo et al.*, 1993; *Takalo and Timonen*, 1998; *Freeman et al.*, 2000; *Hnat et al.*, 2002] and ionospheric convection [*Parkinson*, 2006; *Abel et al.*, 2006, 2007; *Parkinson*, 2008].

[3] It has been argued [e.g., *Freeman et al.*, 2000] that the scale-free structure in the M-I system could occur either as a result of direct driving by a scale-free solar wind, or as a result of some internal process of the system such as Self Organized Criticality (SOC) [*Chang*, 1992] or internal magnetohydrodynamic (MHD) turbulence [e.g., *Borovsky et al.*, 1997]. Both these ideas were invoked by *Abel et al.* [2006] to interpret a spatial analysis of ionospheric plasma velocity measurements. They found that the scaling of the first order structure function is different in the regions of the polar ionosphere on open and closed magnetic field lines, suggesting different sources. Furthermore, the scaling exponent on open field lines was similar to that seen in the solar wind [e.g., *Hnat et al.*, 2005], suggesting direct driving in this region. *Parkinson* [2006] also found similarities between PDFs of temporal ionospheric plasma velocity fluctuations on open field lines and fluctuations in the Akasofu ϵ parameter (with less similarity displayed on closed field lines). Ionospheric velocity fluctuations have been probed further using structure function analysis, comparing observations with predictions coming from descriptions of turbulence based on the Navier-Stokes equations (Kolmogorov K41 turbulence), extensions of this theory to include the effects of a strong magnetic field (Kraichnan-Iroshnikov KI65 turbulence) and various multifractal (intermittent) versions of these models [e.g., *Frisch*, 1995, and references therein]. In this way, *Abel et al.* [2007] showed that the plasma velocity fluctuations in the polar ionosphere are generally consistent with models of intermittent KI65 turbulence.

[4] In this paper we extend this study to investigate how the turbulent structure in the ionosphere depends on the IMF direction and hence on the geometry and effectiveness of magnetic reconnection.

2. Methodology

[5] The methodology used in this study is identical to that employed by *Abel et al.* [2007] with the added condition that the data are subdivided according to the solar wind conditions. Here we describe the method in brief. For full details and justifications of the methods used, see *Abel et al.* [2007].

[6] The SuperDARN radars [*Greenwald et al.*, 1995; *Chisham et al.*, 2007] measure the line-of-sight (LOS) velocity of electron density irregularities in the E and F region ionosphere aligned along the magnetic field **B**. In the F-region these irregularities move at the $\mathbf{E} \times \mathbf{B}$ drift velocity under the influence of the M-I convection electric field **E**. The radars regularly operate in a common mode, in which the radars scan through 16 beam directions differing by 3.25° in azimuth with a beam width of ∼5°. For each beam, LOS velocities are measured for 75 range gates using a pulse length of 300 μs (equivalent to 45 km range separation) and a lag to the first range of 1200 ms (equivalent to 180 km). A complete scan across 16 beams is

[1]British Antarctic Survey, Natural Environment Research Council, Cambridge, UK.

0094-8276/09/2009GL040336

completed in either 60 or 120 s. In this study we use only common mode data measured by the Halley SuperDARN radar in Antarctica during the interval 1996–2003 inclusive. In addition, we only use data from the beam aligned along the geomagnetic meridian (beam 8) so as not to complicate our analysis by combining data from different look directions. We further restrict ourselves to data taken at range gate 10 and higher so as to retain only F-region backscatter for which the LOS velocity is a reliable estimate of the plasma $\mathbf{E} \times \mathbf{B}$ drift velocity. *Abel et al.* [2006] showed that different scaling behavior exists poleward and equatorward of the open-closed magnetic field line boundary (as determined by the C-F spectral width boundary method [*Chisham and Freeman*, 2003]). They also separated the data set into dayside (0900–1300 MLT) and nightside (1800–0200 MLT) sectors. In this study we restrict ourselves to the sector containing most data, i.e., open magnetic field lines in the nightside ionosphere (1800–0200 MLT).

[7] The SuperDARN LOS velocity data are then further separated into eight subgroups according to the IMF direction (following the method of *Chisham et al.* [2009]). That is, each subgroup covers a 45° IMF clock angle region in the GSM Y-Z plane. The IMF clock angle at any time is estimated using Weimer-mapped IMF data from the ACE spacecraft [*Weimer et al.*, 2002]. In order to calculate structure functions that relate best to particular IMF states we restrict our analysis to relatively stable IMF intervals. (This also deals with any problems that occur due to the uncertainty in the mapping of highly-variable IMF data). We require that more than 70% of the IMF data in each half-hour interval is contained within a single clock angle bin, and then assign all ionospheric velocity data from that interval to the corresponding subgroup.

[8] We calculate the first 3 moments, n, of the structure functions, $S_n(l)$, of the LOS velocity differences:

$$S_n(l) = \langle |v(r+l,t) - v(r,t)|^n \rangle \quad (1)$$

where $v(r, t)$ is the LOS velocity measurement made at range r and time t and l is some range separation (in the LOS direction). For each radar scan we identify all pairs of data that are present for a given separation l (where l is an integer multiple of the 45 km range gate separation) and subtract the more equatorward measurement of LOS velocity from the more poleward one ($v(r + l, t) - v(r, t)$) and repeat this for all data from all scans in each clock angle bin from the 8-year period. This set of velocity fluctuations is then conditioned by rejecting all fluctuations larger than three standard deviations, $3\sigma\Delta_v(l)$, from the mean of this distribution [*Abel et al.*, 2007]. We then take the modulus of these values, raise to the power n and average ($\langle |v(r + l, t) - v(r, t)|^n \rangle$). This is repeated for range gate separations from 1 (l = 45 km) to 55 (l = 2475 km). We only show here structure functions of order 3 and less as *Abel et al.* [2007] showed that higher order calculations were unreliable due to velocity measurement aliasing.

3. Results

[9] Figure 1 shows the first three order structure functions plotted as a function of separation calculated using the algorithm presented above for each of the eight IMF clock angle bins. The clock dial in the center of Figure 1 indicates the IMF direction at the center of each bin, and also points toward the plot that relates to that clock angle bin. It should be noted that S_2 has been divided by 200 and S_3 has been divided by 50,000 in order to show them clearly on the same figure as S_1 (it is the shape and slope of the line that we are most interested in, rather than the absolute value). Each of the eight panels has a similar form where each of the three structure functions is a power law (i.e., straight line on a log-log plot) at small separations (<600–1000 km) and deviates from this at large separations (>600–1000 km). The deviation was attributed by *Abel et al.* [2006] to the global 2-cell convection pattern. In support of this, it is interesting to note that the form of the deviation from power law, whilst similar between the three lines in any one plot, varies between the different clock angle directions.

[10] As well as the form of the deviation of S_n from power law at large separation varying with clock angle, the scaling exponents, ζ_n, (i.e., the slopes of the plotted structure functions) also vary. The red lines in Figure 1 show straight lines fitted to the power law regions of each line (using a least-squares fit to the points in log-log space, where the extent of the fit is selected by eye). The scaling exponents of these fitted lines are shown in Figure 2 where the dial plot again indicates the IMF direction at the center of each bin. The error bars shown on the points have been calculated from the variation of ζ_n for conditioning between $2\sigma_{\Delta v}(l)$ and $4\sigma_{\Delta v}(l)$, shown by *Abel et al.* [2007] to be the largest source of error.

[11] Also shown in Figure 2 are three lines. The solid black line shows the values of ζ_n expected for a mono-fractal with a scaling exponent equal to the measured ζ_1 (shown in red), i.e., $\zeta = n\zeta_1$. The dotted red line shows the ζ_n values predicted from the mono-fractal Kraichnan-Iroshnikov (KI65) model of MHD turbulence, i.e., $\zeta = n/3$ (identical in all plots). The solid red line shows the ζ_n values predicted from a multifractal P-model of KI65 turbulence

$$\zeta_n = 1 - \log_2 \left(p^{n/4} + (1-p)^{n/4} \right) \quad (2)$$

with the free parameter p determined from ζ_1. This model was shown by *Abel et al.* [2007] to give the best fit to the total data set (when not discriminating by IMF clock angle). The reason for using ζ_1 to determine the free parameter in the P-model and the slope of the mono-fractal line is that this is the best defined structure function.

[12] By comparing the calculated structure functions to the lines shown in Figure 2, we can make the following statements: (1) The mono-fractal line with a scaling exponent equal to ζ_1 (black) does not describe the data well with the exception of the bin centered around due northward IMF (and possibly the −y −z IMF direction). (2) The mono-fractal KI65 line (dotted red) does not describe the data well for any bin, again with the exception of the bin centered around due northward IMF. (3) The multifractal KI65 line (solid red) describes ζ_1 by definition, but also ζ_2 well for all bins, and ζ_3 to varying degrees. (iv) In the bin centered around due northward IMF all three lines are very similar indicating that ζ_1 is very close to the value of 0.25 predicted by the mono-fractal KI65 turbulence (i.e., the free parameter

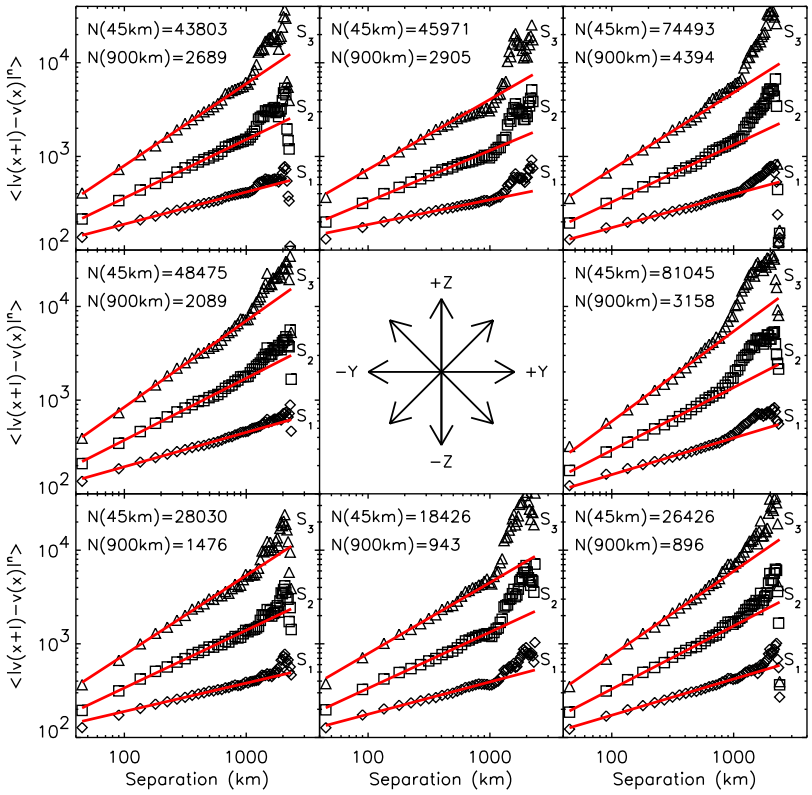

Figure 1. The first three order structure functions (S_1, S_2, and S_3) plotted as a function of separation l (S_1 diamonds, S_2 squares, and S_3 triangles) for the eight IMF clock angle directions. The central direction of each 45° clock angle bin is shown by the dial in the centre of the figure. For convenience S_2 has been divided by 200 and S_3 has been divided by 50,000. The red lines show straight lines fitted to the power law region of each structure function. The figures given in the top left corners indicate the number of data pairs used in the structure function calculation at separations of 45 km and 900 km.

in the multifractal KI65 model is such that the multifractality is very small).

4. Discussion

[13] The results presented above extend the previous findings of *Abel et al.* [2006, 2007]. At scales <1000 km the structure functions are a power law implying scale-free structure that corresponds to the inertial range of turbulence. At larger scales deviations from the power law are seen which have been interpreted as being due to the dominance of the familiar Dungey convection cells. The new fact that the deviation from a power law varies as a function of IMF clock angle supports this view because it is well known that the large scale ionospheric convection varies systematically with IMF clock angle [e.g., *Ruohoniemi and Greenwald*, 2005]. It is worth noting that the scaling exponents found here and by *Abel et al.* [2007] are somewhat larger than those found by *Parkinson* [2008] in similar regions but in the temporal domain. The two studies may be expected to be equivalent when invoking the Taylor hypothesis, i.e., that temporal and spatial scales are equivalent if the flow over the point of observation is fast compared to the changes in the field. However, this is unlikely to be so in the ionosphere and so we suggest therein lies the reason for the discrepancy.

[14] The more significant new result comes from seeing how the scaling exponents ζ_n vary as a function of n for different IMF directions. The IMF clock angle directions in Figure 2 can be split into two groups: the first is when the IMF is directed close to purely northward, and the second is all other IMF directions. The values of ζ_1, ζ_2, and ζ_3 for the purely northward IMF bin are well described by a mono-fractal with a scaling exponent of 0.25. During other IMF conditions they are not. Despite this the structure function scaling exponents may be broadly described for all IMF directions by a single intermittent turbulence model, the multifractal KI65 model, with varying intermittency such that there is zero intermittency for due northward IMF and non-zero intermittency otherwise. This observation is somewhat contradictory to the work of *Parkinson* [2006], who, using data from the Halley and TIGER SuperDARN radars, found temporal scaling exponents not to vary significantly when the data was separated according to whether the IMF B_z was positive or negative. This apparent paradox is likely explained by the fact that we only find mono-fractal structure for the purely northward IMF bin, and the scaling exponents of the other northward IMF bins are indeed similar to the southward IMF bins. Thus *Parkinson* [2006] did not resolve the IMF finely enough to see the difference we have found.

[15] It is well known that during periods of southward IMF the M-I system is strongly coupled to the solar wind

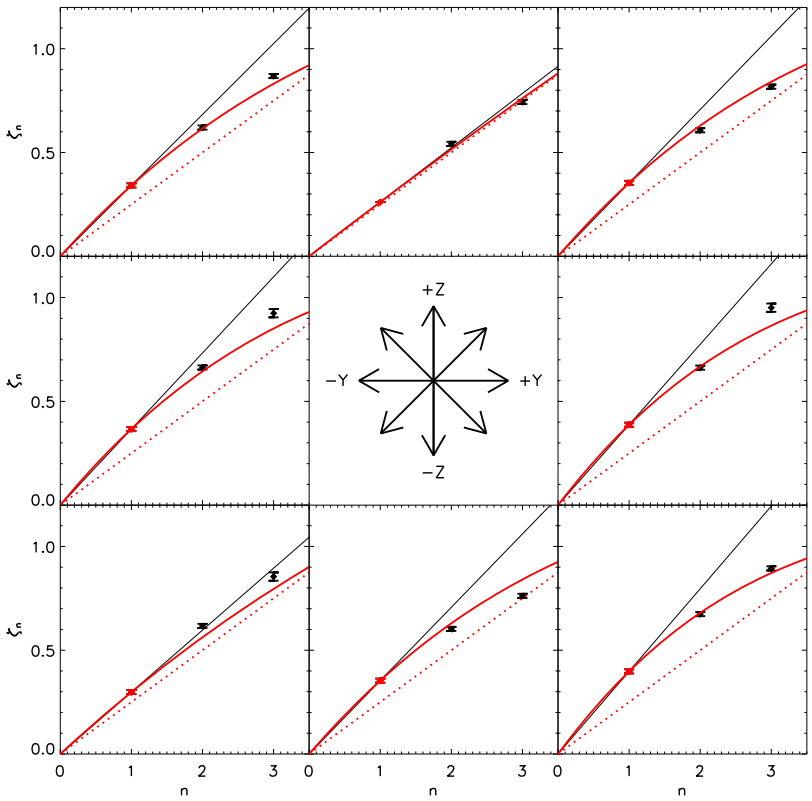

Figure 2. The scaling exponents (ζ_1, ζ_2, and ζ_3) of the first three order structure functions (S_1, S_2, and S_3) for the eight IMF clock angle directions. The central direction of each 45° clock angle bin is shown by the dial in the centre of the figure. Also shown are the values of ζ_n expected for a mono-fractal with a scaling exponent equal to ζ_1 (solid black), the mono-fractal Kraichnan-Iroshnikov (KI65) model of MHD turbulence (dotted red), and a multifractal P-model of KI65 turbulence with the free parameter determined from ζ_1 (solid red).

through magnetic reconnection between the IMF and the magnetospheric field at latitudes equatorward of the cusp, driving a strong 2-cell convection pattern on the system scale [*Dungey*, 1961]. During northward IMF, reconnection can still occur in the lobe regions but no new open flux is added to the magnetosphere and the extent and strength of ionospheric convection is much reduced compared to that seen during southward IMF with often no clear convection pattern, especially in the nightside ionosphere. The transition to lobe cell reconnection does not happen at ±90° clock angle but rather at around ±45° clock angle [e.g., *Freeman et al.*, 1993] coincident with the transition to zero intermittency in ionospheric turbulence. With this basic picture we can suggest various reasons for the variation of multifractality with IMF.

[16] Our favoured interpretation follows that of *Abel et al.* [2006], i.e., that the scale-free structure exhibited in the polar ionospheric plasma flow is inherited from the solar wind driving it. When the M-I system is strongly coupled to the IMF the intermittency in the ionosphere is inherited directly from the solar wind. However, the symmetry of the turbulence is changed as it is transmitted from the solar wind to the ionosphere due to the stronger mean magnetic field. In the solar wind with a relatively weak mean field the turbulence is described by an intermittent K41 model [e.g., *Pagel and Balogh*, 2001], whereas in the ionosphere with a strong mean field it is converted to intermittent KI65 turbulence. In the non-driven case of purely northward IMF the ionosphere is decoupled from the solar wind and ionospheric turbulence is effectively freely decaying and does not inherit any intermittency.

[17] Another possible interpretation is that the intermittency only arises when a global convection pattern is established and arises due to the turbulence being constrained by the size of the system. For example a 2-dimensional numerical simulation of an inverse turbulent cascade showed that intermittency only became present once vortices on the scale size of the simulation were established [*Smith and Yakhot*, 1993]. In this case multifractality need not necessarily come from the solar wind but rather could be inherent to the ionosphere itself.

[18] A third possibility is that the intermittency is inhomogeneous relative to the local mean ionospheric flow direction. The SuperDARN radars measure only the LOS component of the velocity and so the structure function comprises an unknown mixture of longitudinal and transverse fluctuations. During periods of southward IMF there is a strongly defined convection pattern and given the MLT sector under study most measurements made are along the direction of the mean flow. During periods of northward IMF there is no dominant average flow direction (especially in the nightside ionosphere) and so the orientation of our observations is distinctly different for these conditions. However, numerical simulations of turbulence have shown smaller intermittency for longitudinal than for transverse fluctuations [e.g., *Grossmann et al.*, 1997], which would be

in the wrong sense to explain the results shown in this paper.

5. Conclusions

[19] We have presented a structure function analysis of 8 years of LOS ionospheric plasma velocity data measured by the Halley SuperDARN radar sorted according to the IMF clock angle. We find that the plasma velocity fluctuations are consistent with intermittent Kraichnan-Iroshnikov turbulence for all clock angles and that the intermittency decreases to zero during purely northward IMF conditions. We suggest that the intermittency disappears during periods of purely northward IMF as this is when coupling between the solar wind and the magnetosphere/ionosphere effectively switches off, and that thus the intermittency is inherited from the solar wind.

[20] **Acknowledgments.** The authors thank Nick Watkins for useful discussions.

References

Abel, G., and M. P. Freeman (2002), A statistical analysis of ionospheric velocity and magnetic field power spectra at the time of pulsed ionospheric flows, *J. Geophys. Res.*, *107*(A12), 1470, doi:10.1029/2002JA009402.

Abel, G., M. P. Freeman, and G. Chisham (2006), Spatial structure of ionospheric convection velocities in regions of open and closed magnetic field topology, *Geophys. Res. Lett.*, *33*, L24103, doi:10.1029/2006GL027919.

Abel, G., M. P. Freeman, G. Chisham, and N. W. Watkins (2007), Investigating turbulent structure of ionospheric plasma velocity using the Halley SuperDARN radar, *Nonlinear Processes Geophys.*, *14*, 799–809.

Bering, E. A., III, J. R. Benbrook, G. J. Byrne, B. Liao, J. R. Theal, L. J. Lanzerotti, and C. G. Maclennan (1995), Balloon measurements above the South Pole: Study of ionospheric transmission of ULF waves, *J. Geophys. Res.*, *100*, 7807–7819.

Borovsky, J. E., R. C. Elphic, H. O. Funsten, and M. F. Thomsen (1997), The Earth's plasma sheet as a laboratory for flow turbulence in high-β MHD, *J. Plasma Phys.*, *57*, 1–34.

Buchert, S. C., R. Fujii, and K.-H. Glassmeier (1999), Ionospheric conductivity modulation in ULF pulsations, *J. Geophys. Res.*, *104*, 10,119–10,133.

Campbell, W. H. (1976), An analysis of the spectra of geomagnetic variations having periods from 5 min to 4 hours, *J. Geophys. Res.*, *81*, 1369–1390.

Chang, T. (1992), Low-dimensional behavior and symmetry-breaking of stochastic systems near criticality: Can these effects be observed in space and in the laboratory, *IEEE Trans. Plasma Sci.*, *20*, 691–694.

Chisham, G., and M. P. Freeman (2003), A technique for accurately determining the cusp-region polar cap boundary using SuperDARN HF radar measurements, *Ann. Geophys.*, *21*, 983–996.

Chisham, G., et al. (2007), A decade of the Super Dual Auroral Radar Network (SuperDARN): Scientific achievements, new techniques and future directions, *Surv. Geophys.*, *28*, 33–109.

Chisham, G., M. P. Freeman, G. A. Abel, W. A. Bristow, A. Marchaudon, J. M. Ruohoniemi, and G. J. Sofko (2009), The spatial distribution of average vorticity in the high-latitude ionosphere and its variation with interplanetary magnetic field direction and season, *J. Geophys. Res.*, *114*, A09301, doi:10.1029/2009JA014263.

Consolini, G., P. De Michelis, A. Meloni, L. Cafarella, and M. Candidi (1998), Levy-stable probability distribution of magnetic field fluctuations at Terra Nova Bay (Antarctica), paper presented at VIII Workshop on Italian Research on Antarctic Atmosphere, Soc. Ital. di Fis., Bologne.

Dungey, J. W. (1961), Interplanetary magnetic field and the auroral zones, *Phys. Rev. Lett.*, *6*, 47–48.

Francia, P., U. Villante, and A. Meloni (1995), An analysis of geomagnetic field variations (3 min–2 h) at a low latitude observatory (L = 1.6), *Ann. Geophys.*, *13*, 522–531.

Freeman, M. P., C. J. Farrugia, L. F. Burlaga, M. R. Hairston, M. E. Greenspan, J. M. Ruohoniemi, and R. P. Lepping (1993), The interaction of a magnetic cloud with the Earth: Ionospheric convection in the Northern and Southern hemispheres for a wide-range of quasi-steady interplanetary magnetic-field conditions, *J. Geophys. Res.*, *98*, 7633–7655.

Freeman, M. P., N. W. Watkins, and D. J. Riley (2000), Evidence for a solar wind origin of the power law burst lifetime distribution of the AE indices, *Geophys. Res. Lett.*, *27*, 1087–1090.

Frisch, U. (1995), *Turbulence*, Cambridge Univ. Press, Cambridge, U. K.

Greenwald, R. A., et al. (1995), DARN/SuperDARN: A global view of the dynamics of high-latitude convection, *Space Sci. Rev.*, *71*, 761–796.

Grossmann, S., D. Lohse, and A. Reeh (1997), Different intermittency for longitudinal and transverse fluctuations, *Phys. Fluids*, *9*, 3817–3825.

Hnat, B., S. C. Chapman, G. Rowlands, N. W. Watkins, and M. P. Freeman (2002), Scaling of solar wind and the AU, AL, and AE indices as seen by Wind, *Geophys. Res. Lett.*, *29*(22), 2078, doi:10.1029/2002GL016054.

Hnat, B., S. C. Chapman, and G. Rowlands (2005), Scaling and a Fokker-Planck model for fluctuations in geomagnetic indices and comparison with solar wind ϵ as seen by Wind and ACE, *J. Geophys. Res.*, *110*, A08206, doi:10.1029/2004JA010824.

Pagel, C., and A. Balogh (2001), A study of magnetic fluctuations and their anomalous scaling in the solar wind: The Ulysses fast latitude scan, *Nonlinear Processes Geophys.*, *8*, 313–330.

Parkinson, M. L. (2006), Dynamical critical scaling of electric field fluctuations in the greater cusp and magnetotail implied by HF radar observations of *F*-region Doppler velocity, *Ann. Geophys.*, *24*, 689–705.

Parkinson, M. L. (2008), Complexity in the scaling of velocity fluctuations in the high-latitude *F*-region ionosphere, *Ann. Geophys.*, *26*, 2657–2672.

Pulkkinen, A., A. Klimas, D. Vassiliadis, V. Uritsky, and E. Tanskanen (2006), Spatiotemporal scaling properties of the ground geomagnetic field variations, *J. Geophys. Res.*, *111*, A03305, doi:10.1029/2005JA011294.

Ruohoniemi, J. M., and R. A. Greenwald (2005), Dependencies of high-latitude plasma convection: Consideration of interplanetary magnetic field, seasonal, and universal time factors in statistical patterns, *J. Geophys. Res.*, *110*, A09204, doi:10.1029/2004JA010815.

Smith, L. M., and V. Yakhot (1993), Bose condensation and small-scale structure generation in random force driven 2D turbulence, *Phys. Rev. Lett.*, *71*, 352–355.

Takalo, J., and J. Timonen (1998), Comparison of the dynamics of the AU and PC indices, *Geophys. Res. Lett.*, *25*, 2101–2104.

Takalo, J., J. Timonen, and H. Koskinen (1993), Correlation dimension and affinity of AE data and bicolored noise, *Geophys. Res. Lett.*, *25*, 1527–1530.

Weatherwax, A. T., J. T. Rosenberg, L. J. Lanzerotti, C. G. Maclennan, H. U. Frey, and S. B. Mende (2000), The distention of the magnetosphere on May 11, 1999: High latitude Antarctic observations and comparisons with low latitude magnetic and geopotential data, *Geophys. Res. Lett.*, *27*, 4029–4032.

Weimer, D. R., D. M. Ober, N. C. Maynard, W. J. Burke, M. R. Collier, D. J. McComas, N. F. Ness, and C. W. Smith (2002), Variable time delays in the propagation of the interplanetary magnetic field, *J. Geophys. Res.*, *107*(A8), 1210, doi:10.1029/2001JA009102.

G. A. Abel, G. Chisham, and M. P. Freeman, British Antarctic Survey, Natural Environment Research Council, High Cross, Madingley Road, Cambridge CB3 0ET, UK. (gaab@bas.ac.uk; gchi@bas.ac.uk; mpf@bas.ac.uk)